Published in final edited form as:
J Neurochem. 2010 July ; 114(2): 462–474. doi:10.1111/j.1471-4159.2010.06778.x.

TLR2 Activation Inhibits Embryonic Neural Progenitor Cell Proliferation

Eitan Okun[†,*], **Kathleen J. Griffioen**[†,*], **Tae Gen-Son**[†], **Jong-Hwan Lee**[!], **Nicholas J. Roberts**[†], **Mohamed R. Mughal**[†], **Emmette Hutchison**[†], **Aiwu Cheng**[†], **Thiruma V. Arumugam**[‡], **Justin D. Lathia**[†,§], **Henriette van Praag**[†], and **Mark P. Mattson**[†]

[†]Laboratory of Neurosciences, National Institute on Aging Intramural Research Program, Baltimore, Maryland 21224, U.S.A

[‡]School of Biomedical Sciences, University of Queensland, Brisbane, Queensland, Australia

[!]Department of Anatomy, College of Veterinary Medicine, Konkuk University, Seoul 143-701, South Korea

Abstract

Toll-like receptors (TLRs) play essential roles in innate immunity, and increasing evidence indicates that these receptors are expressed in neurons, astrocytes and microglia in the brain, where they mediate responses to infection, stress and injury. To address the possibility that TLR2 heterodimer activation could affect progenitor cells in the developing brain, we analyzed the expression of TLR2 throughout the mouse cortical development, and assessed the role of TLR2 heterodimer activation in neural progenitor cell (NPC) proliferation. TLR2 mRNA and protein was expressed in the cortex in embryonic and early postnatal stages of development, and in cultured cortical NPC. While NPC from TLR2-deficient and wild type embryos had the same proliferative capacity, TLR2 activation by the synthetic bacterial lipopeptides Pam_3CSK_4 and FSL1, or low molecular weight hyaluronan, an endogenous ligand for TLR2, inhibited neurosphere formation *in vitro*. Intracerebral *in utero* administration of TLR2 ligands resulted in ventricular dysgenesis characterized by increased ventricle size, reduced proliferative area around the ventricles, increased cell density, an increase in $PH3^+$ cells and a decrease in $BrdU^+$ cells in the sub-ventricular zone. Our findings indicate that loss of TLR2 does not result in defects in cerebral development. However, TLR2 is expressed and functional in the developing telencephalon from early embryonic stages and infectious agent-related activation of TLR2 inhibits NPC proliferation. TLR2–mediated inhibition of NPC proliferation may therefore be a mechanism by which infection, ischemia and inflammation adversely affect brain development.

Keywords

TLR2; toll-like receptors; cerebral cortex; NPC; NF-*k*B; proliferation

Introduction

The family of mammalian toll-like receptors (TLRs) includes at least 10 members that sense the presence of pathogenic microorganisms and injury-induced endogenous ligands (Wagner

Corresponding Author: Mark P. Mattson, Phone: (410) 558-8463; Fax: (410) 558-8465; mattsonm@grc.nia.nih.gov.
[*]These authors contributed equally to this work.
[§]Current address, Department of Stem Cell Biology and Regenerative Medicine 9500 Euclid Avenue, NE30 Cleveland, Ohio 44195, U.S.A

2006). Activation of TLRs mediates innate immune responses through nuclear factor-κB (NF-κB) and interferon regulatory factor (IRF)-dependent pathways (Akira 2006). IRF-5 is mainly activated following TLR2 activation while other IRFs such as IRF3 are more specific for TLR3 and TLR4 activation (Lee & Kim 2007). Although TLRs are abundant in the immune system, they are also expressed in non-immune cells including brain cells. While TLR expression within the central nervous system was originally believed to be restricted to microglia, recent data indicate that neurons also express functional TLRs 2, 3, 4 and 8 (Okun *et al.* 2008).

Recent findings suggest that neural progenitor cells (NPC) express one or more TLRs which may play roles in normal brain development and responses of the developing brain to infection and injury. TLR4 activation restricts retinal progenitor cell proliferation during the early postnatal period (Shechter et al. 2008). TLR2 and TLR4 are expressed in adult NPC where they exert opposite effects on proliferation and differentiation; TLR2 enhances dentate gyrus neurogenesis, whereas TLR4 inhibits adult NPC proliferation and neuronal differentiation (Rolls et al. 2007). Activation of TLR2 and TLR4 in adult NPC leads to secretion of pro-inflammatory cytokines such as TNF-α (Covacu et al. 2009). However, while TLR2 is abundant within the nervous system (Bsibsi *et al.* 2002, Kielian 2006), the effects of TLR2 activation during embryonic brain development are unknown.

TLR2 is expressed on the plasma membrane and can form heterodimers with either TLR1 or TLR6. In addition, CD14 acts as a co-receptor for TLR2/1 and TLR2/6 heterodimers, while CD36 is a co-receptor for TLR2/6 (Triantafilou et al. 2006). TLR2 can dimerize with TLR1 to recognize triacylated lipopeptides from bacteria, such as Pam_3CSK_4, or with TLR6 to respond to diacylated lipopeptides such as Pam_2CSK_4 or FSL1. These ligands are specific to TLR2, as in the absence of TLR2 they do not have TLR related biological function, however they can still induce signaling in the absence of either TLR1 or TLR6 (Buwitt-Beckmann *et al.* 2005, Buwitt-Beckmann *et al.* 2006). Increasing numbers of endogenous ligands are found to activate TLR2. For example, hyaluronic acid (HA) cleaved by hyaluronidase, generates low molecular weight (LMW)-HA, activating TLR2 and TLR4 (Jiang et al. 2007). Signaling through TLR2 is mediated by the TIR adaptor proteins MyD88 and Mal (also known as TIRAP) resulting in NF-κB activation (Akira 2006).

TLR2 activation has long been known to occur during bacterial infections. Bacterial infection is common during pregnancy, including bacterial vaginosis, and can result in preterm birth, spontaneous abortion and may have long-lasting adverse effects on brain development (Leitich *et al.* 2003, Sorensen *et al.* 2008, Lowe *et al.* 2008). TLR2 can be activated following cerebral ischemia (Tang et al. 2007) and may play a role in pathogenesis of brain abnormalities resulting from intrapartum hypoxia/ischemia (Graham et al. 2008). Here we show that TLR2 heterodimer components are expressed in proliferating cells in the embryonic mouse telencephalon *in vivo* and NPC *in vitro*. Using TLR2-deficient mice and TLR2-specific ligands we show that while in the absence of an exogenous ligand, TLR2 does not alter NPC proliferation in the developing embryo, TLR2 activation increases the number of $PH3^+$ (phospho-histone 3) cells and reduces the number of $BrdU^+$ cells in the ventricular zone resulting in ventricular dysplasia. This suppression of NPC proliferation is specific for TLR2, as co-administration of ligands for other bacterial-sensing TLRs (TLRs 4, 5 and 9) did not modify the inhibitory effect of TLR2 on NPC.

Materials and Methods

Animals and in utero microinjections

Congenic TLR2-deficient mice (TLR2KO) and wild type (WT) mice of the same genetic background (C57BL/6) were purchased from Jackson Laboratories (Bar Harbor, ME) and

were maintained in the National Institute on Aging animal facility under pathogen-free conditions on a 12 h light / 12 h dark cycle with continuous access to food and water. Embryos of different gestational ages were collected from pregnant mice for tissue analysis. NPC neurosphere cultures were prepared using brain tissue from embryos of TLR2KO and WT mice at either E12 or E15 developmental stages. For *in utero* microinjections of TLR2 ligands, timed-pregnant mice (gestational day 15) were anesthetized with isoflurane and a midline laparotomy was performed to expose the uterine horns. The lateral ventricle in the brain of each embryo was visualized with transillumination and the injections were performed using a glass capillary pipette (75–125 μm outer diameter with beveled tip) driven by a Sutter micromanipulator (Sutter Instrument Company, Novato, CA, USA) equipped with 20 μl Hamilton gas-tight syringe. A 1 μl volume of 0.1 μg of Pam_3CSK_4 dissolved in PBS, or PBS alone, was injected. Following intrauterine surgery, the incision site was closed with sutures (4-0, Ethicon, Somerville, NJ) and the mouse was allowed to recover in a clean cage. Mice were sacrificed at 24 and 72 hours after the injection. All procedures were approved by the National Institute on Aging Animal Care and Use Committee.

BrdU injections protocol

E18.5 pregnant dams were BrdU-injected (50 mg/kg) twice with a two-hour delay between injections. BrdU was freshly prepared in PBS with 0.07N NaOH. Two hours after the last injection, the dams were euthanized and embryos were collected for further analysis.

Immunofluoresence

Embryonic brains were fixed in 4% paraformaldehyde in PBS overnight at 4°C and cryoprotected at 4°C in sequential 20%, and 30% sucrose solutions. The brains were embedded in O.C.T. embedding medium (Sakura) and stored at −80°C until coronal sections (10 μm) were prepared using a cryostat. For PCNA staining, antigen unmasking was performed as follows: sections were rehydrated with PBS and incubated for 10 min in 10 mM sodium citrate (pH 6.5) at 80°C. Nonspecific antibody binding was blocked with 10% normal goat serum (Sigma) containing 0.1% Triton X-100 (Amresco). Sections were incubated overnight at 4°C with the relevant primary antibodies, washed with PBS, followed by incubation with the appropriate species-specific Alexa Fluor 488–conjugated IgG (1:1000, Invitrogen) antibodies in the dark at room temperature (RT) for 1h. Sections were counter-stained with DAPI (0.05 mg/ml solution in PBS, Molecular Probes). Slides were mounted using Permafluor mounting solution (Lab vision, Fremont, CA, USA) and kept at 4°C for volumetric analysis and cell counting. For BrdU staining, slices were washed with TBS and incubated in 2N HCl at 37°C for 30 minutes. Slices were then transferred to 0.1M Boric acid (pH 6.5) for 10 minutes at room temperature. Slices were washed in TBS and blocked for 30 minutes in 3% goat serum. Slices were incubated in rat anti- BrdU (1:50, Harlan, USA) for 72 hours at 4°C. Slices were subsequently washed with TBS and the appropriate alexafluor goat anti-rat antibodies were applied. Slices were washed in TBS and mounted in Permafluor. For staining of NPC, E12 NPC plated on polyethyleneimine (Sigma) coated eight-well chamber slides (Nunc), were maintained in culture for 10 d with the medium replenished every 3 days. NPC were then fixed with fixation solution (4% paraformaldehyde, 4% sucrose in PBS) at RT for 10 min, followed by 3 washes in PBS and incubated with primary and secondary antibodies as described above.

The following antibodies were used for immunofluoresence: anti-TLR1 (see Alexopoulou *et al.* 2002; 1:100; Cat# 14-9011, eBioscience (this antibody recognizes the TLR1 epitope in immunofluoresence, but not in paraffin-embedded immunohistochemistry or western blotting); anti-TLR2 (see Dulay *et al.* 2009; 1:100; Cat# ab47840, Abcam); anti-TLR6 (1:100; Cat# sc-5661, Santacruz); anti-Sox2 (see Wang *et al.* 2009; 1:500; Cat# MAB-2018,

R&D systems); anti-S100β (see Markovitz *et al.* 1997; 1:100; Cat# Z0311, DakoCytomation); anti-MAP2 (see Annies *et al.* 2006; 1:100; Cat# ab5392, Abcam); anti-MBP (see Lattanzi *et al.* 2010; 1:100; Cat# MAB386, Chemicon); anti-PCNA (see Lathia *et al.* 2008; 1:200; Cat# ab29, Abcam); anti-KI67 (see Wong *et al.* 2009; 1:100; Cat# ab15580, Abcam); and anti-PH3 (see Lathia et al. 2008; 1:100; Cat# ab5176, Abcam). Specificity of staining for TLR1, 2 and 6 was verified using RAW264 cells (Supplemental Fig. 1A).

Immunohistochemistry

Embryonic brains or whole embryos were fixed in Bouin's solution (Cat# HT10132, Sigma, MI, USA) for 24 hours at room temperature. Embryos were then transferred to a 70% ethanol solution that was replaced every day until solution became transparent. Following that, tissues were immersed at 80%, 85% 90%, 95% and 100% ethanol solutions for 1 hour each. Fixed tissues were then paraffin-embedded and 5 μm thick slices were mounted on poly-L-lysine coated slides. After deparaffinization and hydration through a graded alcohol series, endogenous peroxidase was quenched by incubation with 0.3% peroxide in methanol for 30 minutes. A Citrate buffer (pH 6.0) was applied to the tissue sections for antigen retrieval as needed, and the process was carried out before primary antibody incubations. Thereafter, the slides were incubated with antibodies against TLR2 (1:200 dilution; Cat# ab47840, Abcam) for 24 hours at 4°C. A standard labeled streptavidin-biotin-peroxidase complex (Vector ABC kit; USA) was used to visualize TLR1, TLR2 and TLR6 immunoreactions. Tissues were stained for 5 minutes with 3,3′-diaminobenzidine as the chromogen (Vector, USA) and counterstained with hematoxylin, dehydrated, and cover-slipped. Primary antibodies were omitted in negative controls.

Stereology

Calculations of ventricle volume and the total proliferative area were based on areas obtained by tracing contours around closely matched sections of ventricles in which cell nuclei were stained with the DNA-binding dye DAPI (20 × objective) or around the proliferative area of sections immunostained with PCNA and KI67 antibodies (20× objective). Images were acquired using an Olympus BX51 epifluorescence microscope modified for stereology with a computer-driven motorized stage, a microfire video camera interfaced to a PC equipped with Stereo Investigator 8 software (MicroBrightfield, Inc., Williston, VT, USA). Ventricular volume was measured in three closely matched sagittal sections (spaced 100 mm apart) and an average ventricular volume was calculated. Measurements were performed on five animals in each experimental group. Volume measurements of the proliferative zone were performed between contours surrounding the ventricle and the proliferative area as defined by PCNA and KI67 staining. The borders of proliferative areas were defined at the edge of the continuum of cells positively stained for PCNA or Ki67. Areas with more diffuse cellular staining (that is, near-by cells that were not stained with Ki67 or PCNA antibodies) were considered outside the proliferative area. Measurements were performed in three closely matched sagittal sections (spaced 100 μm apart) and an average volume of the proliferative zone was calculated. The same area was used to quantify cell number and density. Cells were counted in randomly selected 20 μm × 20 μm squares within a 130 μm × 130 μm grid throughout the proliferative area. These parameters were selected based on the minimum area for which cell counts yielded a confidence of variance < 0.1.

Immunoblotting

Brain tissue protein was extracted using a modified RIPA buffer (150 mM sodium chloride, 50 mM Tris-Hcl, pH=7.4, 1 mM ethylenediaminetetraacetic acid, 1% Triton-X100, 1% sodium deoxycholic acid, 0.1% sodium dodecylsulfate) supplemented with protease inhibitor coctail (Cat# 2714, Sigma, MI, USA) and phosphatase inhibitor cocktails 1 and 2

(Cat# P2850 and P5726 respectively, Sigma, MI, USA). Protein concentration was determined using Bradford reagent (BioRad). Proteins in samples (40 μg) were separated by SDS/PAGE (4–12% polyacrylamide gradient gel) and transferred to a nitrocellulose membrane. The membrane was blocked in 5% nonfat milk for 1 h at RT, followed by an overnight incubation at 4°C with primary antibodies: TLR2 (1:1000, Cat# ab47840; Abcam), TLR6 (1:400, Cat# sc-5661; Santacruz), Myd88 (1:1000; Cat# ab2064; Abcam), IRF3 (1:1000, Cat# 4962; Cell Signaling), IRF5 (1:1000, Cat# ab21689; Abcam) and α-Tubulin (1:10,000; Cat# T6074; Sigma) diluted in 1% non-fat milk and 1% Bovine-serum albumin (BSA) in PBS. The membrane was then washed and incubated with a secondary antibody diluted in 1% non-fat milk and 1% bovine-serum albumin (BSA) in PBS for 1 h at RT. Protein bands were visualized using a chemiluminescence detection kit (Pierce Endogen).

Neurosphere cell cultures

NPC from the cortex were propagated as free-floating aggregates to promote proliferation of neural stem and progenitor cells prior to use in experiments. In brief, the dorsal telencephalon from E15 mouse embryos was isolated, mechanically dissociated, and cells were seeded at a density of 200,000/ml in a T75 flask containing Dulbecco's modified Eagle's medium/Ham's F-12 medium supplemented with B27 (1:50; Invitrogen), epidermal growth factor (EGF), and fibroblast growth factor 2 (FGF2) (both at 20 ng/ml; R&D Systems Inc). After neurospheres had grown for 7 days in culture, cells were dissociated using a NeuroCult cell dissociation kit (StemCell Technologies) and plated into 96 wells plates (Nunc) at 2000 cells per well. Neurospheres which formed were counted after 7 days in culture and the average of 10 wells was determined for each experimental condition. Neurosphere forming assays for E15 WT and TLR2KO NPC were performed in triplicate; each replicate consisted of a pool of embryos from one litter. To measure neurosphere diameter, pictures of 10 wells of each experimental condition were taken using a Magnafire camera. Images were then analyzed using ImageJ software (http://rsbweb.nih.gov/ij/). To induce differentiation, growth factors were withdrawn and neurospheres were plated on polyethyleneimine (Sigma) coated dishes. Immunofluoresence in NPC was performed on E12 derived NPC plated on PEI coated dishes. Differentiation of these cells was obtained by EGF and bFGF growth factors withdrawal.

LDH Assay

Conditioned medium from NPC cultures treated with Pam_3CSK_4 or FSL1 were assayed using the LDH (Lactate dehydrogenase) cytotoxicity kit (Roche). Absorbance was read at 540 nm.

Low molecular weight hyaluronan preparation

High molecular weight hyaluronan (HMW-HA) obtained from human umbilical cord (H1504; Sigma, USA) LMW-HA was digested using hyaluronidase (H4272, Sigma, USA) as previously described (Ikegami-Kawai & Takahashi 2002). Briefly, 5 mg/ml HMW-HA in distilled water was incubated with 500 U hyluronidase (50ul in DDW) at 37°C for 48 hrs. Quality of LMW-HA preparations was examined using Alcian-Blue stained-PAGE as previously described (Ikegami-Kawai & Takahashi 2002). Briefly, HMW-HA and LMW-HA were run on a 10% bis-tris gel. Samples were prepared by loading 5 μl of HA samples supplemented with 2.4 μl 2M sucrose in TBE solution. An additional lane running 0.05% bromo phenol blue (BPB) in TBE/0.3M sucrose solution was used to indicate running stage. Gels were run in a cold room under 100V until BPB reached 1 cm from the bottom of the gel. Gels were then stained using 0.05% Alcian blue in 2% acetic acid in water for 30 min in the dark. HMW and LMW HA are visualized as blue bands.

Mitochondrial Activity Assay

NPC were plated on 96-well plates and treated with either Pam_3CSK_4 or FSL-1 for 48 hours. NPC were then incubated with 10 μM Rezasurin Dye (Sigma) for 30 minutes. Fluorescence was measured using 540nm excitation and 590 nm emission wavelengths.

Reverse Transcriptase-Polymerase Chain Reaction (RT-PCR)

Total RNA was isolated using the QiaZol reagent (Qiagen). RNA was then treated with DNAse I to remove contaminating DNA followed by RNA cleanup using RNeasy Minelute cleanup kit (Qiagen). Reverse transcription of RNA to cDNA was carried out using SuperScript III First-Strand Synthesis SuperMix (Invitrogen). For semi-quantitative PCR, the cDNA synthesized was subjected to PCR amplification using Platinum Blue PCR SuperMix (Invitrogen). PCR was performed using PTC-200 (MJ Research) PCR system, DNA was separated in a 1% TBE-agarose gel and the DNA was visualized by ethidium bromide staining. PCR amplification consisted of 30 cycles of 30 s denaturation at 94°C, 30 s annealing and 30 s of elongation at 72°C. For Real-Time PCR reactions, SYBR GREEN PCR Master Mix (Applied Biosystems) was used in a PTC-200 with a Chromo 4 fluorescence detector (BioRad). The following primers were used throughout the study: TLR1: Forward- 5̀ ATG ATT CTG CCT GGG TGA AG 3̀, Reverse- 5̀ TCT GGA TGA AGT GGG GAG AC 3̀, 174bp, annealing temp 53°C), TLR2: Forward- 5̀ CTC CCA CTT CAG GCT CTT TG 3̀, Reverse- 5̀ AGG AAC TGG GTG GAG AAC CT 3̀, 217bp, annealing temp 53°C), TLR6: Forward- 5̀ ACA CAA TCG GTT GCA AAA CA 3̀, Reverse- 5̀ GGA AAG TCA GCT TCG TCA GG 3̀, 128bp, annealing temp 53°C), CD14 (Forward- 5̀ AGG ACT AGA CCT TAG TCA CA 3̀, Reverse- 5̀ GAG TCC AAA AAG GGA TTT CC 3̀, 240bp, annealing temp 51°C), CD36: Forward- 5̀ GCT TGC AAC TGT CAG CAC AT 3̀, Reverse- 5̀ GAG CTA TGC AGC ATG GAA CA 3̀, 290bp, annealing temp 53°C), Myd88: Forward- 5̀ ACT GGC CTG AGC AAC TA 3̀, Reverse- 5̀ CTT CTT TTC TGG GGG TAG GG 3̀, 360bp, annealing temp 54°C). PCRs were normalized against β-actin (Forward- 5̀ TGG AAT CCT GTG GCA TCC ATG AAA C 3̀, Reverse- 5̀ TAA AAC GCA GCT CAG TAA CAG TCC G 3̀, 348 bp, annealing temp 53°C). The following three primers were used in conjunction to amplify TLR2 mRNA that exists in WT, but not TLR2KO animals (Fig. 1A, right panel): 5' CTT CCT GAA TTT GTC CAG TAC A 3'; 5' GGG CCA GCT CAT TCC TCC CAC 3'; 5' ACG AGC AAG ATC AAC AGG AGA 3', 499 bp (WT), 334 bp (TLR2KO), annealing temp 52°C.

Luciferase reporter activity assay

Primary neurospheres obtained from WT and TLR2KO mice were dissociated and plated at 4000 cells/ml. Cells were transfected with NF-κB, AP-1 or Nrf-2 plasmids along with renilla plasmid using Lipofectamin (Invitrogen) according to the manufacturer's recommendation. At 24 h after transfection, luciferase activity was quantified using a Dual-Luciferase-Reporter System (Promega) and normalized to renilla expression. All analyses were performed in triplicate

Statistical Analysis

Experimental results are expressed as mean ± SEM. Statistical comparisons were made with ANOVA, followed by Newman–Keuls post hoc analysis for pairwise comparisons. All statistical analyzes were performed using OriginPro 8.0 software (Northhampton, MA, USA).

Results

TLR2 receptor complex components are expressed in the telencephalon during embryonic and early postnatal development and in cultured embryonic NPC

TLR2 can function as a heterodimer with either TLR1 or TLR6. In addition, both TLR2/1 and TLR2/6 heterodimers use CD14 as a co-receptor, while CD36 is a co-receptor for TLR2/6 alone (Triantafilou et al. 2006). Both TLR2/1 and TLR2/6 require the TIR adaptor protein Myd88 for intracellular signaling. We therefore asked whether the TLR2 receptor, its signaling adaptor protein Myd88 and two TLR related transcription factors, IRF3 and IRF5 are expressed in NPC *in vitro* and *in vivo*. To examine the developmental expression of TLR2 and its signaling components, we first measured levels of mRNAs encoding TLR1, TLR2, TLR6, CD14, CD36 and MyD88 during embryonic and early postnatal development of the cerebral cortex. The mRNAs for TLR1, TLR2, TLR6, CD14, CD36 and Myd88 were all expressed in the cortex of embryos as early as E11. mRNA levels for MyD88 were significantly elevated at P2, mRNA levels for TLR2 were significantly elevated at P5, and mRNA levels of TLR1, TLR6, CD14 and CD36 were greatest at P7 (Fig. 1A, left panel). In the adult cortex, all these genes are expressed even at the absence of TLR2 (Fig. 1A, right panel). Protein levels for TLR2 are expressed at E11–E15, and have a significant sustained increase at later embryonic and postnatal ages (Fig. 1B), a result consistent with the expression levels of TLR2 mRNA. Interestingly, the protein levels of MyD88 were highly and stably expressed during embryogenesis as well as at postnatal stages (Fig. 1B) despite a consistent and significant increase in its mRNA levels (Fig. 1A. left panel). IRF5 is a transcription factor that is recruited by MyD88 following TLR2 activation. Surprisingly, the protein levels of IRF5 consistently decrease during cortical embryogenesis and are significantly lower at postnatal stages P5 and P7 compared to earlier stages (Fig. 1B). Interestingly, the protein levels of IRF3, a transcription factor that is activated following TLR3 and TLR4 (but not TLR2) activation also decrease during cortical embryogenesis between E15 and P7 compared to E11 developmental stages (Fig. 1B), suggesting a developmental role in addition to mediating signaling via TLR2, TLR3 and TLR4. TLR2 is also expressed on proliferating cells in the embryonic SVZ (Fig. 1C). TLR2 is broadly expressed in cells throughout the developing mouse embryo including the brain (Supplemental Fig. 2A). The level of TLR2 immunoreactivity in the SVZ (Fig. 1C) is considerable, but not as great as its levels in immunogenic tissues such as the thymus (Supplemental Fig. 2B) or the spleen (Supplemental Fig. 2C). TLR2 was also relatively strongly expressed in the choroid plexus in the ventricles (Supplemental Fig. 2D), and was absent other tissues such as cartilage (Supplemental Fig. 2E).

Since TLR2 is expressed in the embryonic SVZ brain *in vivo*, we next examined its expression in telencephalic embryonic NPC. The protein expression of TLR1, TLR2 and TLR6 was assessed by immunostaining in SOX2-expressing cultured embryonic NPC. SOX2-expressing NPC were positively stained for TLR2 and TLR6 but not TLR1 (Fig. 2A). Similar to developing cortical tissue, embryonic NPC, as well as NPC-derived differentiated cells that were grown for 10 days in culture express mRNA for TLR1, TLR2 and TLR6 as well as their co-receptors, CD14 and CD36 and the adaptor protein MyD88 (Fig. 2B). Adult hippocampal NPC from TLR2KO mice give rise to a lower percentage of neurons and a higher percentage of astrocytes than their WT counterparts (Rolls et al. 2007). However, it is unknown whether embryonic TLR2-deficient NPC differ from their WT counterparts in their differentiation potential or whether TLR2 activation affects the fate of differentiating NPC. The ability of E15 cortical NPC to give rise to astrocytes, oligodendrocytes and neurons was not compromised by TLR2 deficiency compared to WT NPC (WT and TLR2KO cells respectively: astrocytes ($S100\beta^+$ cells) 11.4% ± 2.1 and 16.7% ± 4.5; neurons ($MAP2^+$ cells) 61.1% ± 4.5 and 59.8% ± 6.3; oligodendrocytes (MBP^+ cells) 10.5% ± 2.6 and 7.2% ± 0.088; Fig. 2C). TLR2 activation of both E12 or E15 derived NPC did not result

in significant changes in differentiation proportions to neurons or astrocytes (E12 derived NPC: $MAP2^+$ cells, 99.5% ± 0.03 vs. 98.5% ± 0.05 in PBS treated cells; $S100\beta^+$ cells, 0.5% ± 0.04 vs. 1.51% ± 0.06 in PBS treated cells; E15 derived NPC: $MAP2^+$ cells, 84.2% ± 5.6 vs. 83.5% ± 4.2 in PBS treated cells; $S100\beta^+$ cells, 23.22% ± 6.9 vs. 20.8% ± 2.1 in PBS treated cells) (Fig. 2D).

Activation of TLR2 heterodimers inhibits NPC proliferation

The presence of TLR3 was recently reported to negatively regulate the proliferative capability of NPC in the developing embryo (Lathia et al. 2008). To determine whether TLR2 also alters NPC dynamics, we asked whether NPC derived from TLR2-deficient embryos exhibit differences in proliferation. No significant difference was observed between TLR2-deficient and WT NPC in both primary (Supplemental Fig. 3A) and secondary (Supplemental Fig. 3B) sphere formation, or in sphere diameter (Supplemental Fig. 3C). In addition, no difference was observed in viability between the cells as measured by mitochondrial activity (Supplemental Fig. 3D) at 7 DIV. Correlated with these *in vitro* observations, no difference is observed between WT and TLR2KO mice in ventricular size, proliferative area size, the number of proliferative cells in the SVZ and in cell density in the SVZ of E16.5 mouse embryos (Supplemental Fig. 3E).

We next examined whether activation of the TLR2 receptor complex altered proliferation of NPC. This was accomplished using the TLR2/6-specific ligand FSL1 (a synthetic lipoprotein from *Mycoplasma salivarium* (Kiura et al. 2006) and the TLR2/1-specific ligand Pam_3CSK_4 (a synthetic bacterial lipopeptide (Patel et al. 2005). NPC activated with Pam_3CSK_4 (1 μg/ml) or FSL1 (1 μg/ml) formed significantly fewer spheres compared to control NPC (80.11 ± 1.43 for Pam_3CSK_4 and 79.51 ± 1.63 for FSL1, both % of control) (Fig. 3A). However, the diameter of the spheres following Pam_3CSK_4 or FSL1 treatment was not reduced (Fig. 3B). Further, the inhibitory effects of Pam_3CSK_4 and FSL1 on sphere formation in WT cells were not correlated with increased toxicity when measured 24 hours following treatment using a LDH release assay (Fig. 3C). The combined treatment of Pam_3CSK_4 and FSL1 revealed an additive effect rather than a synergistic effect on sphere formation (70.42 ± 1.64, % of control) (Fig. 3A). Similar to single ligand treatments, combined administration had no effect on sphere diameter (Fig. 3B) or viability (Fig. 3C). LMW-HA, an endogenous ligand for TLR2 and TLR4 was also tested for its effects on NPC proliferation. LMW-HA produced by digestion of HMW-HA by hyaluronidase showed inhibition of sphere formation at the dose of 1 μg/ml (Supplemental Fig. 4).

During bacterial infections, not only are TLR2 ligands present in the site of infection, but also ligands for other TLRs are present such as the TLR4 ligand lipopolysaccharide (LPS), the TLR5 ligand, flagellin and the TLR9 ligand CpG. We therefore tested whether a combination of these four ligands exacerbates the effect of TLR2 ligands on sphere formation. While activation of TLR2 using Pam_3CSK_4 resulted in significant inhibition of sphere formation, no combination of the ligands for TLR4 (LPS, 1 μg/ml), TLR5 (flagellin, 1 μg/ml) and TLR9 (CpG DNA, 10 μM) increased this effect (Fig. 3D). Similar results were observed following combined treatment with FSL1 (1 μg/ml) and ligands for TLR4, TLR5 and TLR9, data not shown). None of the TLR ligand combination treatments had an effect on the viability of the cells when measured 48 hours following treatment (Supplemental Fig. 5). Depending on the cell type, TLR2 mediates its innate immune responses in part through the activation of transcription factors such as NFκB, AP-1 or Nrf-2. We therefore examined the ability of TLR2 agonists to activate NF-κB in NPC. Both TLR2 ligands significantly induced NFκB promoter activity, and FSL1 administration resulted in a significantly greater induction of the NF-κB promoter than Pam_3CSK_4 (Fig. 3E). These effects were not observed in TLR2KO NPC (Fig. 3E). Interestingly, although reported to activate AP-1 and Nrf-2 transcription factors in other cell types, TLR2 ligands failed to activated either AP-1

(Supplemental Fig. 6A) or Nrf-2 (Supplemental Fig. 6B) in NPC. Interestingly, sulforaphane, an Nrf-2 agonist failed to induce Nrf-2 activation in NPC but did activate Nrf-2 in SH-SY5Y cells (Supplemental Fig. 6B). Consistent with other reports (Akira & Takeda 2004), TLR2 activation induces phosphorylation of Akt in NPC that was evident at 30 minutes and then was reduced at 60 minutes (Fig. 3F).

TLR2 heterodimer activation results in telencephalic dysplasia in embryonic mice

Because TLR2 activation reduced sphere formation of NPC derived from the embryonic brain *in vitro*, we next examined the effect of intracerebral injections of Pam_3CSK_4 and FSL1 on ventricular morphology and numbers of proliferating cells in the periventricular region *in utero*. When injected into the ventricles of E15 WT mouse embryos, Pam_3CSK_4 (0.1 μg in 1 μl of PBS) induced a significant increase in ventricle size, as measured at E16.5 (Supplemental Fig. 7, PBS, 184 ± 43 μm^3*10^{-2}, n=5; Pam_3CSK_4, 283 ± 38 μm^3*10^{-2}, n=5), and further increased by E18.5 (Fig. 4A, B; PBS, 162.88 ± 19.72 μm^3*10^{-2}, n=5; Pam_3CSK_4, 487.51 ± 30.67 μm^3*10^{-2}, n=5). Pam_3CSK_4 administration resulted in a downward trend in the size of the proliferative area at E16.5 (PBS, 410 ± 48.2 μm^3*10^{-3}; Pam_3CSK_4, 350.9 ± 39.3 μm^3*10^{-3}) (Supplemental Fig. 7) and at E18.5 the proliferative area was significantly smaller (PBS, 319.65 ± 8.88 μm^3*10^{-3}; Pam_3CSK_4, 289.19 ± 9.1 μm^3*10^{-3}) (Fig. 4A, B). This decrease was not observed, however, in TLR2KO mice ($p>0.05$, n=5) implying specificity for TLR2 activation in this effect. As a result, cell density in the proliferative area, as determined by Ki67 and PCNA staining was significantly higher in Pam_3CSK_4 treated mice (PBS, 0.0121 ± 0.000213 cells/μm^3; Pam_3CSK_4, 0.0134 ± 0.000125 cells/μm^3) (Fig. 4A, B). At E18.5, no difference was observed in the total number of proliferating cells (PBS, 4313.02 ± 113.44; Pam_3CSK_4 4478.5 ± 110.6), as measured using PCNA or Ki67, however, Pam_3CSK_4 treatment caused a significant decrease in the numbers of $BrdU^+$ cells in the SVZ (PBS, 840.2 ± 20.44; Pam_3CSK_4, 690.5 ± 21.6) (Fig. 4C). Moreover, Pam_3CSK_4 treatment caused a significant two-fold increase in the number of $PH3^+$ cells (cells at M-phase of the cell cycle) (PBS, 77.8 ± 10.19; Pam_3CSK_4, 135.73 ± 10.9) (Fig. 4D) and an increase in the number of $BrdU^-$ $PH3^+$ cells compared to PBS treated mice (Fig. 4E), indicating an increase in the number of cells arrested in their M-phase of the cell cycle prior to the BrdU injection at E18.5. Importantly, in all the parameters we tested following *in utero* injections both at E16.5 as well as E18.5, we did not observe differences between the ipsilateral and contralateral hemispheres (data not shown).

Therefore, activation of heteromeric TLR2 receptors during embryonic development results in increased ventricle size, decreased proliferative area size, an increase in $PH3^+$ cells and a decrease in the numbers of $BrdU^+$ cells. These findings reveal an adverse effect of TLR2 activation during late embryonic development that results in a reduction in the proliferation of cells in the SVZ.

Discussion

Our data show that: 1) TLR2 is expressed in the developing mouse brain and in cultured embryonic NPC. 2) The presence of TLR2 does not influence NPC proliferation both *in vitro* and *in vivo*, whereas its activation inhibits NPC proliferation *in vitro* and decreases cell proliferation *in vivo*. 3) Activation of TLR2 with bacterial ligands *in utero* results in ventricular dysplasia. The lack of a difference in the proliferation rate of NPC from WT and TLR2KO mice, and the similar ventricular size and gross morphology of brains in WT and TLR2KO embryos, suggests that TLR2 signaling does not play a critical role in embryonic brain development under normal conditions. However, we cannot rule out more subtle effects of endogenous TLR2 signaling on the development of cortical cytoarchitecture, or on the behavior of NPC in the adult brain. In a study of adult hippocampal NPC, TLR2 deficiency did not alter the proliferation of NPC, but did affect their phenotypic fate by

increasing the formation of astrocytes at the expense of neurons (Rolls et al. 2007). In contrast, in the present study the absence of TLR2 did not alter the proportion of astrocytes, oligodendrocytes and neurons that differentiate from embryonic NPC. This apparent discrepancy may result from differences in NPC-specific developmental transcriptional changes at embryonic and adult stages, or alternatively from differences between NPC niches in the developing and adult brain. TLR2 activation in differentiating embryonic NPC derived from either E12 or E15 developmental stages does not affect differentiation proportions to neurons or astrocytes, limiting the effects of TLR2 activation in NPC to proliferation inhibition only.

Very little data exist regarding the expression and functions of TLRs in the developing nervous system. TLR8 is abundant in embryonic brain as early as E12, however this expression is limited to sympathetic ganglia and postmitotic migrating cortical neurons and axons and is not present in the proliferating ventricular zone (Ma et al. 2006). In contrast, NPC express TLRs 2, 3 and 4 from early in CNS development (Lathia et al. 2008). TLR3 is transiently increased from early brain development (E12.5) and begins to diminish at E17.5 (Lathia et al. 2008). In contrast, TLR4 maintains relatively constant expression levels throughout neuronal development and into postnatal stages (Lathia et al. 2008). Our data indicate that TLR2 mRNA is expressed at E11 and into postnatal ages *in vivo* as well as in SOX2-expressing NPC *in vitro*. Notably, while both mRNA and protein levels for TLR2 increase during embryogeneis and into postnatal ages, mRNA for MyD88 increases while its protein levels remain constant during embryogenesis and early postnatal stages. This could be due to reduced stability of the mRNA for MyD88, which requires higher levels of the mRNA to maintain high protein expression levels. The increased expression of TLR2 during cortical development was contrasted by the decreased expression of IRF5, a transcription factor that is activated by TLR2, suggesting a developmental role of IRF5 that may be independent of TLR2. Further, we show that TLR2 and its heterodimer partner, TLR6, but not TLR1, are expressed in proliferating cells in the SVZ. The presence of TLR1 mRNA but not protein levels could imply lack of expression, but could also be the result of differences between *in vivo* and *in vitro* growth conditions. We further show that TLR2 is indeed functional and can be activated in response to both exogenous and endogenous TLR2-specific stimuli which results in Akt phosphorylation and activation of the transcription factor NF-κB, in a manner similar to that shown in immune cells. While in earlier developmental stages, the percentage of proliferating cells is greater than in later developmental stages, the changes discussed above observed in embryonic cortical tissue reflect total mRNA and protein levels not only in SVZ proliferating cells, but also in neurons, glia and to a lower extent possibly other cell types.

Emerging findings suggest that TLRs, whether activated by endogenous or exogenous ligands, often act as negative regulators of NPC proliferation and differentiation. TLR4 activation restricts retinal progenitor cell proliferation in early postnatal eye development (Shechter et al. 2008). TLR8 is expressed in the cortex as early as E12, where its activation restricts neurite outgrowth and induces apoptosis in differentiated neurons (Ma et al. 2006). Similarly, activation of TLR3 inhibits neurite outgrowth and causes growth cone collapse (Cameron *et al.* 2007). TLR3 was recently reported to negatively regulate NPC proliferation during early stages of neuronal development and that TLR3 activation with PolyI:C decreases NPC proliferation (Lathia et al. 2008). The absence of functional TLR3 during embryogenesis promotes proliferation of NPC suggesting that TLR3 may be activated by an endogenous ligand. In contrast, we found that elimination of TLR2 neither affects the proliferative capacity of embryonic NPC, nor alters the fate of cells during differentiation *in vitro*. However, similar to TLR3 activation, activation of TLR2/6 or TLR2/1 heterodimers with either FSL1 or Pam_3CSK_4 respectively, or with an endogenous ligand for TLR2, LMW-HA, inhibits NPC proliferation *in vitro*. Therefore, while TLR2 itself may not

participate in restricting NPC proliferation, its activation by either exogenous or endogenous ligands diminishes the proliferative capacity of NPC.

Activation of TLR2 with FSL1, Pam_3CSK_4 or with LMW-HA inhibited neurosphere formation *in vitro* and caused ventricular dysplasia when injected into the ventricles of E15 mouse embryos as indicated by a significant increase in ventricle size, decrease in the proliferative area, increase in cell density in the proliferative area, an increase in the number of $PH3^+$ cells and a decrease in the number of $BrdU^+$ cells in the SVZ. This suggests that TLR2 activation interferes with the cell cycle of NPC, prevents cells from incorporating BrdU and prevents them from exiting M-phase of the cell cycle, thereby causing telencephalic dysplasia. The mechanism for these effects could involve both direct actions on the NPC and indirect effects. Indirect effects could result from an increase in cell density followed by cellular stress leading to deleterious counter effects, or also ventricular edema induced by TLR2 signaling in ependymal cells could cause ventricular volume increase, which culminates in decreased SVZ volume. Interestingly, there were no significant changes in all the tested parameters following *in utero* injection between the ipsilateral and contralateral embryonic hemispheres. This could be due to either a rapid dispersion of Pam_3CSK_4 throughout the embryonic CNS or as suggested above, due to an extrinsic effect such as a released factor(s) that culminate in telencephalic dysplasia.

Despite the high degree of specificity of TLR2/1 and TLR2/6 heterodimers to their ligands, we did not observe any differences in the effects conferred by the two ligands. Equimolar doses of both TLR2/6 and TLR2/1 activation induced comparable rates of neurosphere formation inhibition. TLR2 stimulation results in NF-κB activation in macrophages (Schwandner et al. 1999), AP-1 in gastric cells (Chang et al. 2005) and Nrf-2 in tracheal smooth muscle cells (Lee et al. 2008). Inhibition of NPC proliferation by both ligands was correlated with NF-κB promoter activity but not AP-1 or Nrf-2. While FSL1 administration resulted in greater NF-κB promoter activity compared to Pam_3CSK_4, FSL1 was not more potent than Pam_3CSK_4 in inhibiting NPC proliferation, suggesting that the increase evoked by Pam_3CSK_4 was sufficient to maximally inhibit NPC proliferation. In addition, the basal activity of AP-1 was not affected by either TLR2 ligands, and no promoter activity of Nrf-2 was observed in NPC even in response to sulforaphane, an Nrf-2 activator (Ellis 2007). Moreover, co-administration of Pam_3CSK_4 and FSL1 resulted in a significant but mild additive inhibitory effect, which likely results from mutual downstream signaling induced by the two ligands.

Our findings are of interest in the context of alterations in brain development caused by infectious agents, ischemia and inflammatory states. TLR2 activation has long been known to occur in immune cells during bacterial infections. Bacterial infection is common during pregnancy, including bacterial vaginosis, and can result in preterm birth and spontaneous abortion (Leitich et al. 2003, Sorensen et al. 2008). Prenatal infection can also have profound lasting effects on brain development. For example, maternal bacterial infection is correlated with increased risk of schizophrenia (Sorensen et al. 2008). Maternal infection with lipopolysaccharide (LPS), a TLR4 agonist, is associated with altered hippocampal morphology and decreased synaptic transmission (Golan *et al.* 2005, Lowe et al. 2008). LPS administration results in cerebral death and sensitizes the developing chick brain to hypoxic damage and death (Wang et al. 2008). Further, prenatal LPS infection selectively reduces baseline numbers of dopaminergic neurons in the substantia nigra, thereby increasing the vulnerability of the animals to a Parkinsonian toxin (6-hydroxydopamine) later in life (Ling et al. 2004). Our findings suggest that *in utero* exposure of the brain to infectious agents that produce TLR2 ligands or endogenous activation of TLR2 such as those used in the present study may diminish the proliferative capacity of embryonic NPC and possibly lead to lasting abnormalities of neuronal plasticity and behavior. One particularly interesting long-term

effect is whether TLR2-mediated telencephalic dysplasia affects the rostral migratory stream of NPC to the olfactory bulb, and whether this culminates in behavioral abnormalities in the adult mouse.

Supplementary Material

Refer to Web version on PubMed Central for supplementary material.

Acknowledgments

We thank Dr. Michelle Potter for technical assistance, Dr. Uri Ashery for critical comments on the manuscript and Dr. Simonetta Camandola for kindly supplying plasmids for NF-κB, AP-1 and Nrf-2 luciferase reporter assays. The authors declare no conflicting interests.

Abbreviations used in the text

TLR	Toll-like receptors
NPC	Neuronal progenitor cells

References

Akira S. TLR signaling. Curr Top Microbiol Immunol. 2006; 311:1–16. [PubMed: 17048703]

Akira S, Takeda K. Toll-like receptor signalling. Nature reviews. 2004; 4:499–511.

Alexopoulou L, Thomas V, Schnare M, Lobet Y, Anguita J, Schoen RT, Medzhitov R, Fikrig E, Flavell RA. Hyporesponsiveness to vaccination with Borrelia burgdorferi OspA in humans and in TLR1- and TLR2-deficient mice. Nature medicine. 2002; 8:878–884.

Annies M, Bittcher G, Ramseger R, Loschinger J, Woll S, Porten E, Abraham C, Ruegg MA, Kroger S. Clustering transmembrane-agrin induces filopodia-like processes on axons and dendrites. Molecular and cellular neurosciences. 2006; 31:515–524. [PubMed: 16364653]

Bsibsi M, Ravid R, Gveric D, van Noort JM. Broad expression of Toll-like receptors in the human central nervous system. J Neuropathol Exp Neurol. 2002; 61:1013–1021. [PubMed: 12430718]

Buwitt-Beckmann U, Heine H, Wiesmuller KH, Jung G, Brock R, Akira S, Ulmer AJ. Toll-like receptor 6-independent signaling by diacylated lipopeptides. European journal of immunology. 2005; 35:282–289. [PubMed: 15580661]

Buwitt-Beckmann U, Heine H, Wiesmuller KH, Jung G, Brock R, Akira S, Ulmer AJ. TLR1- and TLR6-independent recognition of bacterial lipopeptides. The Journal of biological chemistry. 2006; 281:9049–9057. [PubMed: 16455646]

Cameron JS, Alexopoulou L, Sloane JA, et al. Toll-like receptor 3 is a potent negative regulator of axonal growth in mammals. J Neurosci. 2007; 27:13033–13041. [PubMed: 18032677]

Chang YJ, Wu MS, Lin JT, Chen CC. Helicobacter pylori-Induced invasion and angiogenesis of gastric cells is mediated by cyclooxygenase-2 induction through TLR2/TLR9 and promoter regulation. J Immunol. 2005; 175:8242–8252. [PubMed: 16339564]

Covacu R, Arvidsson L, Andersson A, Khademi M, Erlandsson-Harris H, Harris RA, Svensson MA, Olsson T, Brundin L. TLR activation induces TNF-alpha production from adult neural stem/progenitor cells. J Immunol. 2009; 182:6889–6895. [PubMed: 19454685]

Dulay AT, Buhimschi CS, Zhao G, Oliver EA, Mbele A, Jing S, Buhimschi IA. Soluble TLR2 is present in human amniotic fluid and modulates the intraamniotic inflammatory response to infection. J Immunol. 2009; 182:7244–7253. [PubMed: 19454721]

Ellis EM. Reactive carbonyls and oxidative stress: potential for therapeutic intervention. Pharmacol Ther. 2007; 115:13–24. [PubMed: 17570531]

Golan HM, Lev V, Hallak M, Sorokin Y, Huleihel M. Specific neurodevelopmental damage in mice offspring following maternal inflammation during pregnancy. Neuropharmacology. 2005; 48:903–917. [PubMed: 15829260]

Graham EM, Ruis KA, Hartman AL, Northington FJ, Fox HE. A systematic review of the role of intrapartum hypoxia-ischemia in the causation of neonatal encephalopathy. Am J Obstet Gynecol. 2008; 199:587–595. [PubMed: 19084096]

Ikegami-Kawai M, Takahashi T. Microanalysis of hyaluronan oligosaccharides by polyacrylamide gel electrophoresis and its application to assay of hyaluronidase activity. Anal Biochem. 2002; 311:157–165. [PubMed: 12470675]

Jiang D, Liang J, Noble PW. Hyaluronan in tissue injury and repair. Annu Rev Cell Dev Biol. 2007; 23:435–461. [PubMed: 17506690]

Kielian T. Toll-like receptors in central nervous system glial inflammation and homeostasis. J Neurosci Res. 2006; 83:711–730. [PubMed: 16541438]

Kiura K, Kataoka H, Nakata T, Into T, Yasuda M, Akira S, Inoue N, Shibata K. The synthetic analogue of mycoplasmal lipoprotein FSL-1 induces dendritic cell maturation through Toll-like receptor 2. FEMS Immunol Med Microbiol. 2006; 46:78–84. [PubMed: 16420600]

Lathia JD, Okun E, Tang SC, et al. Toll-like receptor 3 is a negative regulator of embryonic neural progenitor cell proliferation. J Neurosci. 2008; 28:13978–13984. [PubMed: 19091986]

Lattanzi A, Neri M, Maderna C, di Girolamo I, Martino S, Orlacchio A, Amendola M, Naldini L, Gritti A. Widespread enzymatic correction of CNS tissues by a single intracerebral injection of therapeutic lentiviral vector in leukodystrophy mouse models. Human molecular genetics. 2010

Lee IT, Wang SW, Lee CW, Chang CC, Lin CC, Luo SF, Yang CM. Lipoteichoic acid induces HO-1 expression via the TLR2/MyD88/c-Src/NADPH oxidase pathway and Nrf2 in human tracheal smooth muscle cells. J Immunol. 2008; 181:5098–5110. [PubMed: 18802114]

Lee MS, Kim YJ. Signaling pathways downstream of pattern-recognition receptors and their cross talk. Annual review of biochemistry. 2007; 76:447–480.

Leitich H, Bodner-Adler B, Brunbauer M, Kaider A, Egarter C, Husslein P. Bacterial vaginosis as a risk factor for preterm delivery: a meta-analysis. Am J Obstet Gynecol. 2003; 189:139–147. [PubMed: 12861153]

Ling ZD, Chang Q, Lipton JW, Tong CW, Landers TM, Carvey PM. Combined toxicity of prenatal bacterial endotoxin exposure and postnatal 6-hydroxydopamine in the adult rat midbrain. Neuroscience. 2004; 124:619–628. [PubMed: 14980732]

Lowe GC, Luheshi GN, Williams S. Maternal infection and fever during late gestation are associated with altered synaptic transmission in the hippocampus of juvenile offspring rats. Am J Physiol Regul Integr Comp Physiol. 2008; 295:R1563–1571. [PubMed: 18753265]

Ma Y, Li J, Chiu I, et al. Toll-like receptor 8 functions as a negative regulator of neurite outgrowth and inducer of neuronal apoptosis. J Cell Biol. 2006; 175:209–215. [PubMed: 17060494]

Markovitz NS, Baunoch D, Roizman B. The range and distribution of murine central nervous system cells infected with the gamma(1)34.5- mutant of herpes simplex virus 1. Journal of virology. 1997; 71:5560–5569. [PubMed: 9188630]

Okun E, Griffioen KJ, Lathia JD, Tang SC, Mattson MP, Arumugam TV. Toll-like receptors in neurodegeneration. Brain Res Rev. 2008

Patel M, Xu D, Kewin P, Choo-Kang B, McSharry C, Thomson NC, Liew FY. TLR2 agonist ameliorates established allergic airway inflammation by promoting Th1 response and not via regulatory T cells. J Immunol. 2005; 174:7558–7563. [PubMed: 15944255]

Rolls A, Shechter R, London A, Ziv Y, Ronen A, Levy R, Schwartz M. Toll-like receptors modulate adult hippocampal neurogenesis. Nat Cell Biol. 2007; 9:1081–1088. [PubMed: 17704767]

Schwandner R, Dziarski R, Wesche H, Rothe M, Kirschning CJ. Peptidoglycan- and lipoteichoic acid-induced cell activation is mediated by toll-like receptor 2. J Biol Chem. 1999; 274:17406–17409. [PubMed: 10364168]

Shechter R, Ronen A, Rolls A, London A, Bakalash S, Young MJ, Schwartz M. Toll-like receptor 4 restricts retinal progenitor cell proliferation. J Cell Biol. 2008; 183:393–400. [PubMed: 18981228]

Sorensen HJ, Mortensen EL, Reinisch JM, Mednick SA. Association Between Prenatal Exposure to Bacterial Infection and Risk of Schizophrenia. Schizophr Bull. 2008

Tang SC, Arumugam TV, Xu X, et al. Pivotal role for neuronal Toll-like receptors in ischemic brain injury and functional deficits. Proc Natl Acad Sci U S A. 2007; 104:13798–13803. [PubMed: 17693552]

Triantafilou M, Gamper FG, Haston RM, Mouratis MA, Morath S, Hartung T, Triantafilou K. Membrane sorting of toll-like receptor (TLR)-2/6 and TLR2/1 heterodimers at the cell surface determines heterotypic associations with CD36 and intracellular targeting. The Journal of biological chemistry. 2006; 281:31002–31011. [PubMed: 16880211]

Wagner H. Endogenous TLR ligands and autoimmunity. Adv Immunol. 2006; 91:159–173. [PubMed: 16938540]

Wang Q, He W, Lu C, Wang Z, Wang J, Giercksky KE, Nesland JM, Suo Z. Oct3/4 and Sox2 are significantly associated with an unfavorable clinical outcome in human esophageal squamous cell carcinoma. Anticancer research. 2009; 29:1233–1241. [PubMed: 19414369]

Wang X, Carmichael DW, Cady EB, Gearing O, Bainbridge A, Ordidge RJ, Raivich G, Peebles DM. Greater hypoxia-induced cell death in prenatal brain after bacterial-endotoxin pretreatment is not because of enhanced cerebral energy depletion: a chicken embryo model of the intrapartum response to hypoxia and infection. J Cereb Blood Flow Metab. 2008; 28:948–960. [PubMed: 18030303]

Wong SY, Seol AD, So PL, Ermilov AN, Bichakjian CK, Epstein EH Jr. Dlugosz AA, Reiter JF. Primary cilia can both mediate and suppress Hedgehog pathway-dependent tumorigenesis. Nature medicine. 2009; 15:1055–1061.

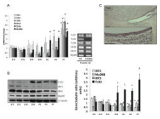

Figure 1.

TLR2 receptor is expressed in the brain cortex during development. **A**. (left panel) Real-Time PCR analysis of TLR1, TLR2, TLR6, CD36, CD14 and Myd88 at different embryonic and early post-natal developmental stages. (right panel) PCR analysis of the same genes in adult (8 weeks old) WT and TLR2KO mice. * P<0.05 compared to E11–E19 developmental stages. # p<0.05 compared to E11-P5 developmental stages. (Two-way ANOVA) **B**. (left panel) Immunoblots of TLR2, IRF3, IRF5 and MyD88 proteins in the developing cortex. (right panel) densitometric analysis of protein levels normalized to α-tubulin levels. § p<0.05 compared to E11–E15 developmental stages. ‡ p<0.05 compared to E11-P5 developmental stages. * p<0.05 compared to E11 developmental stage. ¶ p<0.05 compared to E11 developmental stage (Two-way ANOVA). For each developmental stage, n=3. **C**. Saggital section showing immunostaining for TLR2 with hematoxilin counterstaining in the SVZ of an E15 embryo. Scale bar = 200 μm. Scale bar of inset images = 50 μm. V; ventricle.

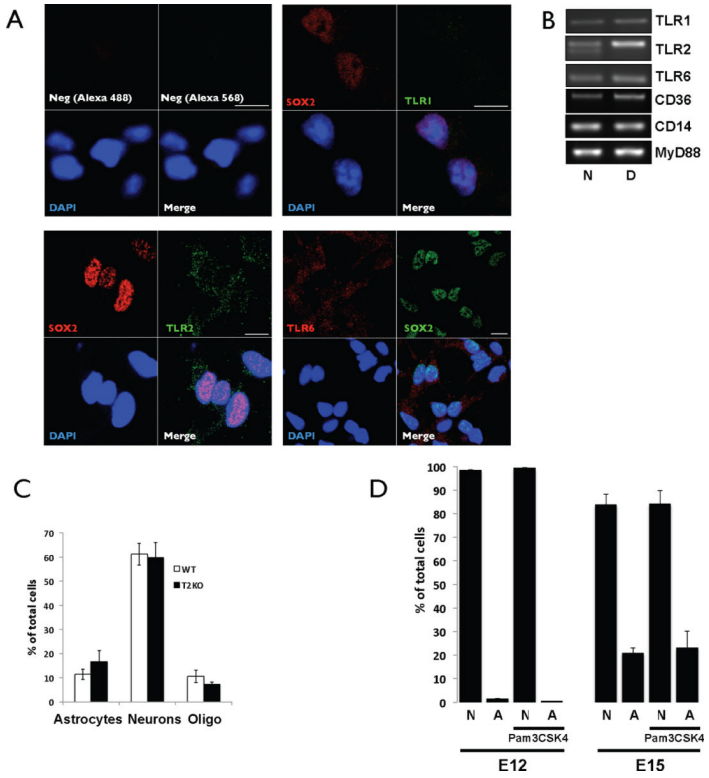

Figure 2.

TLR2 receptor mRNA and protein is expressed in cultured embryonic NPC. **A**. $SOX2^+$ Embryonic NPC *in vitro* express TLR2 and TLR6, but not TLR1. **B**. Representative PCRs for TLR1, TLR2, TLR6, CD36, CD14 and Myd88 mRNA expression in NPC (N) and differentiated NPC (D). **C**. No difference is observed between E15 TLR2KO and WT NPC in their differentiation capacity. The graph shows percentage of astrocytes, neurons and oligodendrocytes differentiated from E15.5 derived NPC (values are the mean and SEM; n = 3 experiments). **D**. While E15 derived NPC give rise to fewer neurons and more glial cells compared to E12 derived NPC, TLR2 activation using Pam_3CSK_4 does not change the differentiation ratio into neurons (N, determined by $MAP2^+$ staining) or astrocytes (A, determined by $S100\beta^+$ staining) in both E12 and E15 derived NPC. Scale bar = 10 μm.

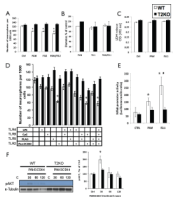

Figure 3.

TLR2 activation inhibits neurosphere formation. **A**. Sphere formation is reduced following Pam_3CSK_4 and FSL1 administration, while the combined administration of both ligands results in a mild additive effect. (A–F, Open bars WT, Filled bars TLR2KO) **B and C**. Pam_3CSK_4, FSL1 or their combination does not alter neurosphere diameter (B) or viability of cells (C) in the neurospheres. **D**. Inhibition of neurosphere formation is specific for TLR2. Administration of LPS, CpG, Flagellin, Pam_3CSK_4 or any combination of these ligands did not enhance the inhibition of neurosphere formation induced by Pam_3CSK_4 alone. **E**. Pam_3CSK_4 and FSL1 significantly increase NF-κB activation in NPC. **F**. (left panel) Pam_3CSK_4 activation results in rapid phosphorylation of AKT at 30 minutes in WT but not TLR2KO cells. (right panel) Densitometric analysis of AKT phosphorylation. (For all graphs the values are the mean and SEM; n = 5 experiments). *$p<0.05$ compared to control; #$p<0.05$ compared to Pam_3CSK_4 (Two-way ANOVA). Legend refers to all graphs.

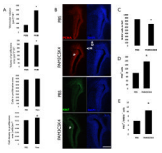

Figure 4.

TLR2 heterodimer activation *in utero* at E15 results in telencephalic dysplasia at E18.5. **A**. Pam_3CSK_4 (0.1 μg in 1 μl PBS, n=5) injection but not PBS (n=5), significantly enlarges ventricles. The proliferative area, as visualized using Ki67 and PCNA staining significantly decreased while cell density significantly increased following Pam_3CSK_4 administration. No difference was observed in the total number of cells labeled with PCNA or Ki67. **B**. Representative example of ventricular and proliferative area measurements taken from 10 μm coronal brain sections from a PBS treated control embryo and a Pam_3CSK_4 treated embryo. Contours were drawn around the ventricle according to DAPI staining (blue), and around the proliferative area according to the PCNA (red) or Ki67 (green) immunostaining. **C**. Pam_3CSK_4 (0.1 μg in 1 μl PBS, n=5) injection but not PBS (n=5), significantly decreases the number of $BrdU^+$ cells in the SVZ. **D**. Pam_3CSK_4 (0.1 μg in 1 μl PBS, n=5) injection but not PBS (n=5), significantly increases the number of $PH3^+$ cells in the SVZ. **E**. Pam_3CSK_4 (0.1 μg in 1 μl PBS, n=5) injection but not PBS (n=5) increases the ration of $PH3^+/BrdU^-$ cells in the SVZ. P, proliferative zone; V, ventricle; D, dorsal; M, midline. Scale bar represents 300 μm.